GEOPHYSICAL RESEARCH LETTERS, VOL. 26, NO. 8, PAGES 1093-1096, APRIL 15, 1999

Phase-space electron holes along magnetic field lines

L. Muschietti, R. E. Ergun, I. Roth, and C. W. Carlson

Space Sciences Laboratory, University of California, Berkeley

Abstract. Recent observations from satellites crossing active magnetic field lines have revealed solitary potential structures that move at speeds substantially greater than the ion thermal velocity. The structures appear as positive potential pulses rapidly drifting along the magnetic field. We interpret them as BGK electron holes supported by a population of trapped and passing electrons. Using Laplace transform techniques, we analyse the behavior of one phase-space electron hole. The resulting potential shapes and electron distribution functions are self-consistent and compatible with the field and particle data associated with the observed pulses. In particular, the spatial width increases with increasing amplitude. The stability of the analytic solution is tested by means of a two-dimensional particle-in-cell simulation code with open boundaries. We also use our code to briefly investigate the influence of the ions. The nonlinear structure appears to be remarkably resilient.

1. Introduction

Satellites exploring the magnetospheric plasma have several times reported the observation of solitary potential structures. Besides negative potential pulses, which have been known for a while [*Temerin et al.*, 1982], fast-moving pulses with the opposite polarity are now being observed. The best data are collected by the FAST satellite and its high-resolution plasma and field instruments in the downward-current regions of the auroral zone. The observed potential structures [*Ergun et al.*, 1998a] have a large enough amplitude to modulate the entire electron distribution function (up to $e\Phi > T_e$, or $\sim$ 100 Volts), move along the magnetic field opposite to the current with a speed of 500–5000 km/s, and have a parallel size of a few Debye lengths. The speed is significant insofar as it is much larger than the ion thermal velocity, and on the order of the electron drift. In fact, the electromagnetic signature of a potential pulse may be described as that of a traveling electron hole. Similar solitary structures have been observed by the Polar satellite at higher altitudes in the auroral zone: at 2 R_E [*Mozer et al.*, 1997] (S.R. Bounds, private communication, 1998) as well as at 5–7 R_E [*Franz et al.*, 1998; *Cattell et al.*, 1998]. They were first identified by the Geotail satellite in the plasma sheet boundary layer as the constituents of the broadband electrostatic noise [*Matsumoto et al.*, 1994; *Omura et al.*, 1996], and since then have also been spotted at bow shock crossings [*Matsumoto et al.*, 1997; *Bale et al.*, 1998].

After analysing several hundred potential spikes from the FAST dataset, it was concluded [*Ergun et al.*, 1998b] that a Gaussian provides a reasonably good fit to their spatial shape in the parallel direction. The existence and stability of such a potential form requires a particular inhomogeneous electron distribution: there must be a depleted phase-space density in the region of the spike and this electron hole must be self-supporting.

The plasma environment of the spikes observed by FAST is collisionless, has a Debye length of order 100 m, and is strongly magnetized with a gyro-to-plasma frequency ratio of $\Omega_e/\omega_e \sim 5 - 15$. Because the electrons are tightly tied to a magnetic field line, their one-dimensional dynamics is what mainly determines the observed potential spike.

In this paper, we construct a one-dimensional BGK solution [*Bernstein et al.*, 1957; *Turikov*, 1984] which displays the characteristics of the observed potentials and electron distributions. We test its stability by loading it as initial condition in a 2-D, non-periodic, electrostatic, particle-in-cell code. Exploiting an open-boundary design, we perform the simulations in the frame of the potential spike and investigate the effect of the ions, which appear in this frame as a cold beam impinging upon the BGK structure with a large kinetic energy.

2. Solitary wave as localized BGK electron hole

To describe a nonlinear solitary structure, it is customary to distinguish between the particles which are trapped in the frame of the structure, or interact strongly, from those which just pass it and interact weakly. The measured distributions [*Carlson et al.*, 1998] reflect mostly the characteristics of the passing electrons since a potential spike passes by the FAST satellite in 100 μs while the compilation of an electron distribution takes $\sim$80 ms. These distributions are broad in the parallel direction, flat-topped, and drifting with an average speed larger or comparable to that of the solitary structures [*Ergun et al.*, 1998b]. By contrast, the information about the trapped electrons is much less clear. Cuts in the distributions, available on a much shorter time scale, display strong modulations at the passage of a potential spike. These modulations can be described

Paper number 1999GL900207.
0094-8276/99/1999GL900207$05.00

as a brief broadening accompanied by a decrease in the plateau. We will show below that they can be interpreted naturally within our BGK model.

Working in the frame that moves with the solitary spike, we assume a steady state for both potential and electron distribution. Let f_t, f_e, be the distribution functions of respectively the trapped and the passing electrons, and let $\phi(x)$ be the potential profile along the ambient magnetic field. Poisson equation leads to

$$g(\phi) \equiv \int_{-\phi}^{0} \frac{f_t(w)}{\sqrt{w+\phi}} dw = \frac{d^2\phi}{dx^2} - \int_0^{\infty} \frac{f_e(w)}{\sqrt{w+\phi}} dw + 1 . \quad (1)$$

The distribution functions are written in terms of the constant of motion $w = v^2 - \phi$ (normalized energy), so that the stationary Vlasov equation is satisfied. Energy is normalized by $mv_e^2/2$ where $v_e = \sqrt{T_e/m}$ is the electron velocity spread, distance is normalized by the Debye length $\lambda_d = v_e/\omega_e$, and potential is normalized by $T_e/2e$. The terms on the RHS are supposedly known from a proper modelling of the FAST observations. The last term $(+1)$ represents the neutralizing ions, which we assume to be unaffected. By contrast, the LHS, formally defined as $g(\phi)$, is largely unknown.

Note from (1) that there are two contributions to $g(\phi)$: one that originates from the shape of the potential, $(d^2\phi/dx^2)$, and one from the charge imbalance between passing electrons and neutralizing background, $(1-\int_0^{\infty} f_e(w)(w+\phi)^{-1/2}dw)$. Noting that the unknown function $f_t(w)$ is defined over the half space $w < 0$, we use the Laplace transform to invert (1). In Laplace space the convolution integral of the LHS becomes a simple product, enabling us to extract $f_t(w)$:

$$f_t(w) = \frac{1}{\pi} \int_0^{-w} \frac{1}{\sqrt{-w-\phi}} \frac{d}{d\phi} g(\phi)\, d\phi . \quad (2)$$

In reaching (2) the property $g(\phi) \to 0$ for $\phi \to 0_+$ has been used.

From the observations [*Ergun et al.*, 1998b] we assume the potential profile parallel to the magnetic field to fit a Gaussian of width δ and amplitude ψ

$$\phi(x) = \psi \exp(-0.5\, x^2/\delta^2) . \quad (3)$$

The following model emulates qualitatively the measured electron distributions while keeping the calculations simple:

$$f_e(w) = \frac{6\sqrt{2}}{\pi(8+w^3)} . \quad (4)$$

This describes a distribution function that is at rest in the frame of the potential spike, is flat-topped for $v \lesssim 1$, and drops as a power law at larger velocities. Using (4) to integrate the second term in the RHS of (1) where $\phi = 0$, one can check that the density is normalized to unity, which cancels exactly the ion contribution.

Performing the integral in (2) with the help of (3) and (4) to evaluate $g(\phi)$, we find the self-consistent distribution of trapped electrons,

$$f_t(w) = \frac{6 + (\sqrt{2}+\sqrt{-w})(1-w)\sqrt{-w}}{\pi(\sqrt{2}+\sqrt{-w})(4-2w+w^2)} + \frac{2\sqrt{-w}}{\pi\delta^2}\left[1 + 2\ln(\frac{\psi}{-4w})\right] \quad \text{with } -\psi \le w < 0. \quad (5)$$

The term on the first line, which is positive, comes from the passing electrons, whose density naturally thins as they are accelerated about the positive potential. The term on the second line comes from the potential profile and is very sensitive to the width δ. It is negative near the hole center, $w \to -\psi$, becomes positive at the periphery, and vanishes for $w \to 0_-$. The density depletion between hole center and periphery corresponds to the curvature difference of ϕ at its peak and on its flanks. Since the term contributes negatively to $f_t(w)$ near $w \gtrsim -\psi$, it is clear that too small a δ can lead to unphysical solutions for the distribution function of deeply trapped electrons.

In the limit $w \to 0_-$ one obtains $f_t \to 3/(2\sqrt{2}\pi)$, which matches continuously with the passing distribution f_e from (4). An illustration in (x, v) space of the complete distribution function

$$F(w) = \begin{cases} f_t(w), & \text{if } w < 0 \\ f_e(w), & \text{if } w > 0 \end{cases} \quad (6)$$

is given in Figure 1. $F(w)$ is continuous at the separatrix, $w = 0$. Note the way F looks as a function of v: strongly depleted around $x = 0$ where the solitary potential is centered, and flat-topped for positions away from it. Note also how F bulges where the potential is large. This feature translates into a brief broadening of electron distributions observed in the spacecraft frame when a potential spike passes by. Because the drift speed is a fraction of the velocity spread, this may result in a reverse flux of energetic electrons being observed in the spacecraft frame, as seen in the FAST dataset.

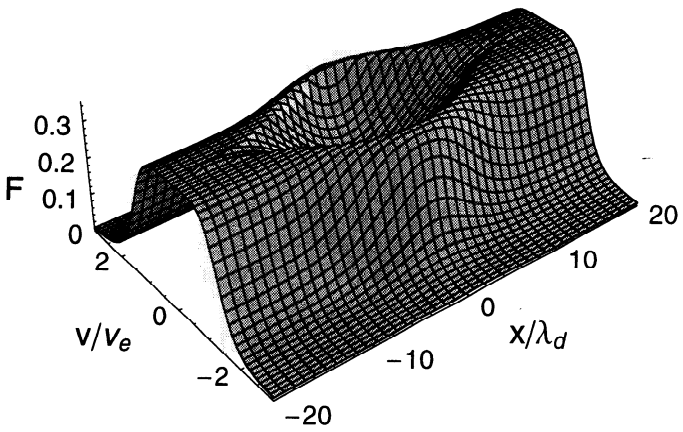

Figure 1. Distribution function in (x, v) space exhibiting an electron hole. Perspective view made from (6) with $w = v^2 - \phi(x)$. The associated potential is centered on $x = 0$ with a width $\delta = 5\ \lambda_d$. As a function of v, the flat-top distribution bulges and becomes core depleted at the potential spike.

The solitary potential spike is maintained by a deficit of deeply trapped electrons. The distribution function f_t, however, cannot be negative at its minimum for $w = -\psi$. This imposes a relation between width δ and amplitude ψ. Substituting $w \to -\psi$ in (5) we find

$$\delta^2 \geq \sqrt{\psi}(\sqrt{2}+\sqrt{\psi})\frac{(8\ln 2 - 2)(4 + 2\psi + \psi^2)}{6 + \sqrt{\psi}(\sqrt{2}+\sqrt{\psi})(1+\psi)}. \quad (7)$$

We note that $\delta \sim \psi^{1/4}$ for $\psi \ll 1$ and $\delta \sim \psi^{1/2}$ for $\psi \gg 1$. The width must increase for increasing amplitudes [*Turikov*, 1984]. A plot of the relation rescaled in physical units is displayed with a solid line in Figure 2. This behavior differs from a classic soliton, where the larger is the amplitude, the narrower is the structure. The solitary waves discussed in this paper are different nonlinear objects, for which the dominant role is played by the dynamics of the trapped electrons.

Figure 2 displays (points with error bars) the relation between amplitude and size as observed by FAST [*Ergun et al.*, 1998b] besides the relation predicted by the BGK analysis (solid line). Over 1000 solitary structures from 30 different orbits were binned by size. The size is the Gaussian half-width normalized to the local Debye length. The average potential in each bin is normalized to the local electron temperature. The error bars are dominated by uncertainty in the velocity measurement, which is approximately a factor of two. The large uncertainty in velocity observations has two effects. First, it tends to reduce the curvature in the relation as predicted by (7). Next, since the velocity is derived from the inverse of delay time, a large uncertainty results in a net change in the statistical mean. Properly accounting for this uncertainty in the observations is very difficult. Instead, we modify the expected relationship as predicted by (7) for the large uncertainty in delay times, which yields the light dashed line. One can see that the observations quantitatively agree with the predicted size amplitude relation of a one-dimensional BGK structure.

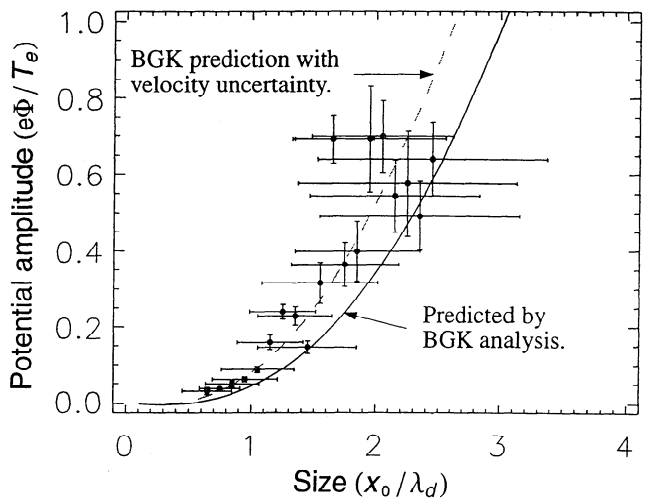

Figure 2. Width-amplitude relation. Statistical determination from the FAST dataset vs prediction for a BGK electron hole. See text for details.

The BGK scheme admits a variety of potential profiles and it is not *a priori* certain that the analytically constructed electron hole is dynamically stable. In order to investigate its stability and evolution, we perform a series of two-dimensional particle simulations. Although the presence of a strong magnetic field restricts the electron motion to one dimension, opening another channel of interaction with oblique waves allows to more critically test the stability of the BGK structure.

It is assumed that a potential spike with specific characteristics has been formed and co-exists with the trapped and passing electrons as described above. The simulation is performed in the frame of the spike, which enables us to follow its evolution over long times in a finite system. Along the coordinate x (parallel to the magnetic field) we impose open boundary conditions. At both ends of the simulation box, we inject electrons with a constant flux determined by $f_e(w = v^2)$ (see (4)), while the exiting electrons are removed from the system. In the perpendicular direction y we impose periodic boundary conditions. Inside the system, the loading along x of the particles at $t = 0$ reproduces the spatially inhomogeneous distribution of electrons described above. The required correlation between space and velocity is obtained by means of the invariant w. A large number of particles per Debye square is used. This keeps the noise level low, allows for good diagnostic, and is essential to produce a smooth injection at the boundaries. Typically, we load 2^{10} particles per Debye square at $t = 0$. Their total number in the system is allowed to fluctuate in time via realistic losses and gains through the boundaries; the resulting potential fluctua-

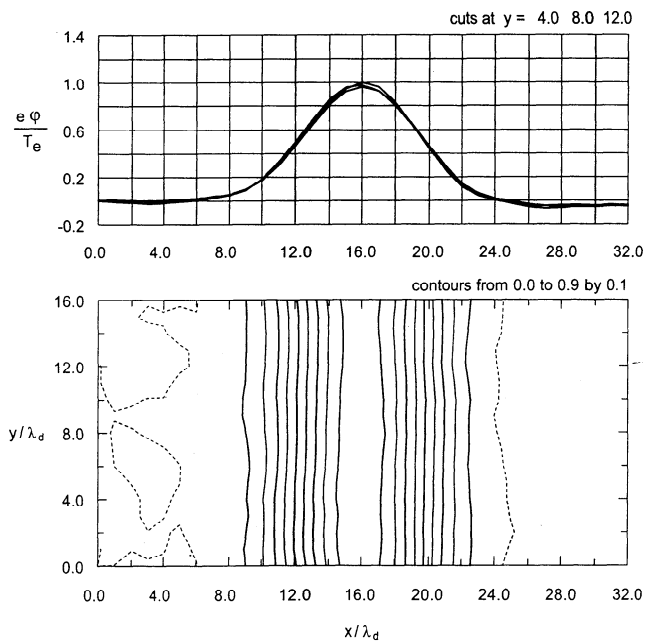

Figure 3. Typical potential structure recorded during the 2-D PIC simulations. (Bottom) Ten contours in (x, y) plane from 0.0 (dotted) to 0.9. (Top) Three cuts at various y, the coordinate perpendicular to the magnetic field. Except for small fluctuations, the potential spike maintains its one dimensional character and is very stable.

tions at the boundaries are calculated from the current integrated over the system.

In a first series of simulation runs the ions form just a homogeneous background. An example of potential structure is shown in Figure 3. The bottom panel gives the contours of $\phi(x, y)$ while the upper panel displays cuts at three different y locations. The potential spike is found to preserve its one-dimensional character and to be very stable. Runs of 10^3 steps, or $\omega_p t = 100$, and with an enlarged box of $128\lambda_d \times 32\lambda_d$ yield very similar results. In order to clarify the microphysics taking place, we tag all the electrons trapped initially (i.e. satisfying $w < 0$ at $t = 0$) and follow them in the contracted phase space $(x - v_x)$. They remain in a clump, which demonstrates that the electron hole forms an entity by itself.

The effect of the ions on the stability of the electron hole depends on their relative energy vs the potential energy of the spike. Since the spike moves with a velocity which is a sizeable fraction of the electron velocity spread, the ions appear in the frame of the spike as a cold beam impinging onto the solitary potential with considerable kinetic energy. Specifically, their energy w is 2 – 3 orders of magnitude larger than that of a typical passing electron ($w \sim 1$). Therefore, in energy terms, the potential spike represents only a small perturbation for the ions, which results in a brief and weak interaction. A second series of simulations varying the relative speed between ions and electron hole show no observable effect on the stability of the latter as long as the speed satisfies $V_r \geq 60\sqrt{\Phi}$ km/s where Φ is the potential in Volts. The simulations also demonstrate that, contrary to expectations based on some analytical calculations [*Maslov and Schamel,* 1993], no growth of the potential spike takes place.

3. Conclusion

The existence, stability, and evolution of spatially-coherent potential structures along magnetic field lines are of general interest for the understanding of magnetized plasmas. As the present study shows, the fast-moving potential spikes observed by satellites on active field lines are in many aspects consistent with the picture of a phase-space electron hole carried by a drifting electron population. First, they have the polarity of a positive potential pulse. Hence, the associated bipolar signature of the parallel electric field is such that the first excursion points toward the electron drift. Second, the measured variations of the energetic electrons at the passage of a potential spike are consistent with our calculations of the electron distribution associated with an electron hole. Third, a statistical study of the solitary spikes show their parallel size to increase with increasing amplitudes, which is precisely the behaviour expected from the potential associated with an electron hole. Finally, the investigation of the interaction between the potential spike and the ions shows that the stability of the former requires a fast-moving structure. This is consistent with the observational fact that slow-moving potential spikes have the opposite polarity and hence must be attributed to ion holes.

Acknowledgments. The simulations were performed on the Cray T90 of the San Diego Supercomputer Center. The work was supported by NASA grants NAG5-3596, NAG5-4898, NAG5-6985, NAG5-2815, and NAG5-3182.

References

Bale, S. D. et al., Bipolar electrostatic structures in the shock transition region: Evidence of electron phase space holes, Geophys. Res. Lett., *25,* 2929, 1998.

Bernstein, I. B., J. M. Greene, and M. D. Kruskal, Exact nonlinear plasma oscillations, *Phys. Rev. 108,* 546, 1957.

Carslon, C. W. et al., FAST observations in the downward auroral current region: Energetic upgoing electron beams, parallel potential drops, and ion heating, Geophys. Res. Lett., *25,* 2017, 1998.

Cattell, C.A. et al., Comparisons of Polar satellite observations of solitary wave velocities in the plasma sheet boundary and the high altitude cusp to those in the auroral zone, Geophys. Res. Lett., *26,* 425, 1999.

Ergun, R. E. et al., FAST satellite observations of large-amplitude solitary structures Geophys. Res. Lett., *25,* 2041, 1998a.

Ergun, R. E. et al., Debye-scale plasma structures associated with magnetic-field-aligned electric fields, Phys. Rev. Lett., *81,* 826, 1998b.

Franz, J. R., P. M. Kintner, and J. S. Pickett, POLAR observations of coherent electric field structures, Geophys. Res. Lett., *25,* 1277, 1998.

Maslov, V. and H. Schamel, Growing electron holes in drifting plasmas, *Phys. Lett. A178,* 171, 1993.

Matsumoto, H. H. et al., Electrostatic solitary waves (ESW) in the magnetotail: BEN wave forms observed by GEOTAIL, Geophys. Res. Lett., *21,* 2915, 1994.

Matsumoto, H. H. et al., Plasma waves in the upstream and bow shock regions observed by Geotail, *Adv. Space Res., 20,* 683, 1997.

Mozer, F. S. et al., New features of time domain electric-field structures in the auroral acceleration region, Phys. Rev. Lett., *79,* 1281, 1997.

Omura, Y., et al., Electron beam instabilities as generation mechanism of electrostatic solitary waves in the magnetotail, J. Geophys. Res., *101,* 2685, 1996.

Temerin, M., et al., Observations of double layers and solitary waves in the auroral plasma, Phys. Rev. Lett., *48,* 1175, 1982.

Turikov, V. A., Electron phase space holes as localized BGK solutions, *Phys. Scr. 30,* 73, 1984.

C. W. Carlson, R. E. Ergun, L. Muschietti, and I. Roth, Space Sciences Laboratory, University of California, Berkeley, CA 94720-7450 (e-mail: laurent@ssl.berkeley.edu)

(Received January 28, 1999; accepted March 1, 1999.)